15TH IEA HEAT PUMP CONFERENCE
MAY 26–29, 2026 | HOFBURG
VIENNA 2026
DECARBONISATION THROUGH INNOVATION

Dynamic model development for large-scale heat pumps to assess their operating characteristics as part of energy systems

Paavo Taipale[a] , Antti Uusitalo[a], Teemu Turunen-Saaresti[a]

[a]LUT University, Yliopistonkatu 34, Lappeenranta 53850, Finland

Abstract

The ongoing electrification of industrial heat production has made the use of heat pumps an attractive and efficient solution for generating heat, while also providing opportunities for significant greenhouse gas emission reductions. Moreover, heat pumps can offer increased flexibility to power systems, a feature that is increasingly important as the EU electricity market transitions from longer trading intervals to shorter ones—such as moving from hourly to fifteen-minute periods. To investigate the dynamic behavior and flexibility of different types of heat pump systems, the development of accurate dynamic models is essential. In this study, a dynamic model for a large-scale heat pump was generated using the Simscape environment in MATLAB Simulink. The aim of the modelling is to provide preliminary information on system dynamics, and it can be utilized in assessing the system's capability for flexible usage. The model is based on an existing industrial-scale heat pump system that produces heat to a district heating network. The study presents the main features of the model, and it also presents a comparison of modelled results to the measured values for the low temperature cycle of the two-stage heat pump. As a result, a simple model was developed, and the simulated results show adequate agreement with the corresponding steady-state measurements. Dynamic operation was also modelled by varying refrigerant mass flow during the simulation which the model handled successfully.

Keywords: Heat pump; Dynamic; Simscape; Modelling

1. Introduction

Achieving full decarbonization and reaching net-zero greenhouse gas emissions by 2050 is a major climate objective for the European Union [1]. In the energy sector and in many industrial sectors, the reliance on fossil fuels to produce heat has been steadily decreasing, as a growing share of heat is generated through the conversion of electricity [2]. This electrification of heat production not only accelerates the decarbonization of the heating sector but can also improve the overall energy efficiency. Technologies capable of electrifying heating systems at both small- and large-scale, such as heat pumps and electric boilers, utilize electricity for heat production. Therefore, their emission profile depends on the source of the electricity that is used [3]. Additionally, heat pump technology can harness low-grade industrial waste heat as an energy source, raising its temperature to a usable level and thereby enabling the recovered heat to be reused within industrial processes.

The increasing integration of renewable energy sources—such as wind and solar power—into electricity generation is further declining the use of fossil fuels. However, the variable nature of renewables introduces uncertainty into electricity grids, as the availability of wind and solar power fluctuates with weather conditions. To maintain the necessary balance between electricity production and consumption, improved operational flexibility in the electric grid is essential. One promising method to provide this flexibility is the use of heat pumps in industrial heat production. During periods of surplus electricity generation, heat pumps can operate to store excess heat in thermal storage systems. This stored heat can then be utilized for industrial processes or other heating networks during times of electricity deficit, thereby reducing the need for electricity consumption when the electricity supply is limited.

To be able to understand the degree of flexibility that is achievable via heat pumps the dynamic performance characteristics of heat pumps need to be studied. Flexible heat pump usage would track the electric grid changes and vary its operational behavior accordingly. In addition, demand response management and control strategies with heat pumps considering the real time electricity pricing has been investigated e.g. [4]. Regarding the response time of systems for load changes, heat pumps being physical systems they are not capable of instantaneously adjusting the heating capacity from 0 to 100 % operation, because they demand certain ramping times which are dependent on the components. The response time for the capacity changes is dependent on the heat exchanger types and mass, compressor specifications, inertia of the fluid and thermal mass of the piping. In energy systems, the inertia of the heat exchangers has been observed to be the most significant factor affecting the system response times under changing load conditions [5-6].

Dynamic models and modelling methods suitable for heat pumps have been developed and investigated previously. Many of these studies have focused on smaller scale heat pumps, such as use of heat pumps in household heating [7-8]. Industrial large-scale heat pump dynamic modelling has also been studied in some instances [9-10]. For this kind of simulation of heat pumps, different modelling tools can be used. One often used tool is Modelica [8-10]. Another well-known simulation tool option, which hasn't perhaps been as commonly used with heat pump simulations, is MATLAB's Simscape [11-12].

This study focuses on dynamic modelling and developing dynamic models for a large-scale heat pump. A heat pump system that is utilized for district heating production serves as a case example. The study presents the main features of a dynamic model of heat pump cycle. MATLAB's Simulink Simscape application was selected as the platform for realizing the model. The model includes the basic heat pump components which are modelled with the readily available Simscape component library. The main components required to model the cycle are the compressor, evaporator, condenser, and the expansion valve.

2. Methods

2.1. Case

Simscape, an addition to Simulink software in MATLAB is used in generating the heat pump model. The simulated case is an existing heat pump facility. The facility produces heat to the district heating network in the municipality of Lempäälä, Finland. The system is owned by Lempäälän Lämpö oy and it can be considered as a so-called smart energy system, as the facility utilizes different kinds of heat production methods, such as heat pumps and CHP gas engines. The heat pump system is a cascade heat pump combined by two heat pump cycles with an intermediate cycle between them. The system can provide both heating and cooling. The heat pump uses R1234ze(E) as the refrigerant. In the intermediate cycle and in the heat sink cycle water is used as the heat transfer fluid whereas in the heat source cycle, ethylene glycol water mixture (35%) is used. The system is divided into two heat pumps, one low temperature cycle and one high temperature cycle. The whole cascade system is not modelled here, as the simulation model is made only for the low-temperature cycle of the heat pump. Simplified illustration of the system is shown in Fig. 1.

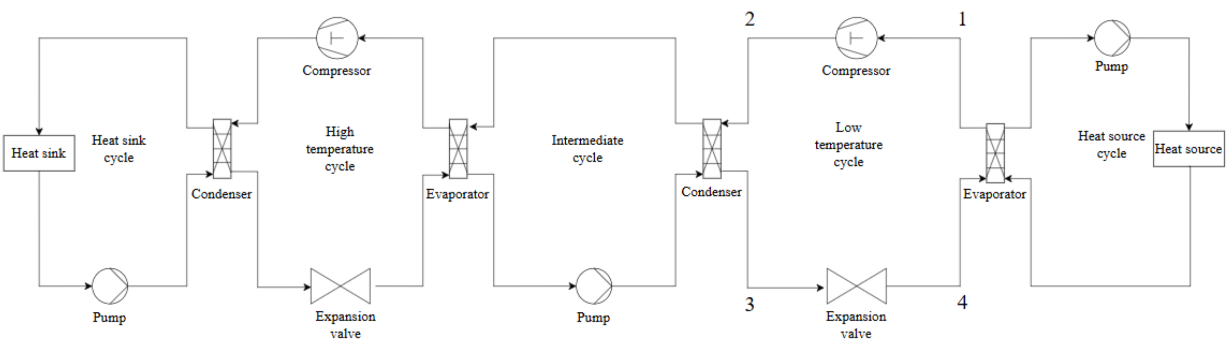

Figure 1. Simple illustration of the cascade heat pump system.

Because the focus of this study is on the low temperature cycle, we will go through its details more in depth next. Components included in the heat pump cycle are a plate evaporator, four compressors connected in parallel, plate condenser, expansion valve, internal heat exchanger (IHX) and a subcooler. In the chosen stationary state of the low temperature cycle, the heat source temperature is 22.4 °C and heat sink flow is heated to 48.9 °C. Heating and cooling powers are 390 kW and 290 kW respectively. Total compressor mechanical power is 99 kW. Pressure before the compressors is 2.7 bar(a) and after 10 bar(a).

The thermodynamic property database Coolprop [13] was used for defining the properties of the refrigerant that are required in the simulations. The properties were imported to Simscape by using 'Two-phase fluid properties' -block. The pressure and internal energy range were set with certain amount of data points between them. The ranges and number of data points used are shown in Table 1.

Table 1. Fluid property settings

Quantity	Unit	Value
Minimum pressure	0.1	bar
Maximum pressure	100	bar
Minimum specific internal energy	100	kJ/kg
Maximum specific internal energy	650	kJ/kg
Number of pressure data points	250	-
Number of specific internal energy data points	200	-

The modelling methods, important equations, and detailed description of the main components in the cycle, such as the compressor and heat exchangers are presented in the following subsections. Information of the components is from Simscape documentation [14].

2.2. Compressor

The investigated system utilizes positive displacement type of compressors. Therefore, the compressor behaviour was modelled by using the 'Positive-Displacement Compressor (2P)' -block in the heat pump model. Even though the system has four compressors, now a simplification is done and only one compressor block is used representing the total compressor capacity of the four individual compressors in the real system. For the compressor, the nominal conditions need to be defined into the block parameters as they are used in determining the behaviour of the compressor. These nominal parameters include mass flow rate, shaft speed, pressure ratio, inlet pressure and inlet temperature. The compressor displacement volume is calculated by using the given nominal values according to Eq. (1).

$$V_{disp} = \frac{\dot{m}_{nom} v_{nom}}{\omega_{nom} \eta_{V,nom}} \tag{1}$$

The volumetric efficiency is determined analytically as shown in Eq. (2)

$$\eta_V = 1 + C - C\left(\frac{v_{in}}{v_{out}}\right) \tag{2}$$

The constant 'C' in this case means clearance volume fraction.

$$C = \frac{1 - \eta_{V,nom}}{\frac{v_{in,nom}}{v_{out,nom}} - 1} \tag{3}$$

The real mass flow rate is calculated with Eq. (4).

$$\dot{m} = \eta_V \omega \frac{V_{disp}}{v} \tag{4}$$

Corresponding continuity equations are shown in Eq. (5) and (6).

$$\dot{m}_{in} + \dot{m}_{out} = 0 \tag{5}$$

$$\dot{E}_{in} + \dot{E}_{out} + \dot{m}_{in}\Delta h_t = 0 \tag{6}$$

Fluid power achieved from compressor is the third term in the previous Eq. (6).

$$P_f = \dot{m}_{in}\Delta h_t \tag{7}$$

2.3. Heat exchangers and pipe connections

Simscape has multiple different types of heat exchangers available, out of which the ‘Plate Condenser Evaporator (TL-2P)’ block was selected to be used as evaporator and condenser. Main reason for the choice to use this block is its simplicity and the reason that in the heat pump case the heat exchangers are plate heat exchangers. The block utilizes the effectiveness-NTU method and heat exchangers have the counter-current flow arrangement. The heat exchanger block has two inlets and two outlets corresponding to the inlets and outlets of the two fluids. To be able to predict the behavior of the heat exchangers, certain geometry specifications are required for the heat exchanger blocks. The required specifications include the number of plates, plate width and length, as well as the spacing of the plates. Additionally, the increase in surface area resulting from the plate surface patterns is accounted for by using a 'surface area enlargement factor.

The total amount of refrigerant in the whole system is determined in the components that include fluid, such as the heat exchangers in this case. The amount depends on the volume determined in specifying heat exchanger geometry and also in the ‘initial two-phase fluid vapor quality’ box. As the cycle is closed, the mass of refrigerant stays the same throughout the simulations.

Volume of the refrigerant inside a heat exchanger can be calculated from Eq. (8). Total volume inside the heat exchanger is the refrigerant volume times two, as then the other heat transfer fluid is also considered.

$$V_{refr} = \frac{(N_p + 1) b L_p W_p}{2} \tag{8}$$

Heat transfer surface area for one fluid side is shown in Eq. (9).

$$A_f = \phi N_p L_p W_p \tag{9}$$

Pressure losses of both fluid sides are calculated by considering Darcy friction factor and the loss coefficient at flow entry and outlet ports. They are given into the calculations as constants, and their values are set as the default values already in the block. The pressure loss between a port – either inlet or outlet – and an internal calculation node inside the heat exchanger is calculated with Eq. (10).

$$p_{port} - p_i = \frac{\xi_{port}\dot{m}_{port}|\dot{m}_{port}|}{4\rho S^2{}_{port}} + \frac{f L_p \dot{m}_{port}|\dot{m}_{port}|}{4\rho D_h S^2} \tag{10}$$

The equations used for convective heat transfer changes depending on the fluid phase. In pure liquid and vapor phases Nusselt number is calculated with Eq. (11).

$$Nu = c_1 (f Re^2 \sin(2\beta))^{c_2} Pr^{c_3} \tag{11}$$

The above-mentioned equation includes β, which is the chevron angle on plate surface corrugation. However, the chevron angle is not chosen as the area enlargement factor is used instead. It is unclear from Simscape documentation how the equation is then calculated in this situation. For two-phase flows Eq. (12) is used.

$$Nu = \frac{c_1 \phi Re_{SL}^{c_2} Pr_{SL}^{c_3} \left\{ \left[\left(\sqrt{\frac{v_{SV}}{v_{SL}}} - 1 \right) x_{out} + 1 \right]^{1+c_2} - \left[\left(\sqrt{\frac{v_{SV}}{v_{SL}}} - 1 \right) x_{in} + 1 \right]^{1+c_2} \right\}}{(1 + c_2) \left(\sqrt{\frac{v_{SV}}{v_{SL}}} - 1 \right) (x_{out} - x_{in})} \tag{12}$$

The convective heat transfer coefficient is then calculated with Eq. (13).

$$U = Nu\frac{k}{D_h} \tag{13}$$

The coefficient is used in calculating total thermal resistance between the heat transfer fluids. Only convective heat transfer is considered in thermal resistance as thermal conductivity through plates and the fouling are ignored.

Heat exchanger geometries were chosen so that they would be similar to the heat exchangers used in the real facility. The fluid volume is defined to be as close as possible, but the heat transfer area was adjusted in order to reach high enough heat flow rate in heat exchangers. This adjustment could also have been done by keeping the heat transfer area comparable to the test facility and by tuning the parameters for example in the Nusselt number correlation.

The IHX was modelled with the ‘pipe (2P)’- blocks. One block was set before the compressor and one before the expansion valve. These two blocks were then connected with a thermal line, in which a constant heat flow rate was set. This heat flow rate value was set as 11 kW which was estimated from temperature change in the measured data. The subcooler was modelled similarly with a ‘pipe (2P)’-block and its heat flow rate was set as 5 kW and its location is set after the condenser and before the IHX. This constant heat flow rate is a simplification for the model, as in real situation the rate would vary as changes occur in the system.

The two-phase pipe block was also used as pipe connections between the components. The exact geometry of the pipes in the system was not considered in this model, so all the pipes’ lengths were set as an arbitrary value of 3 m with inside diameter of 6 cm. No heat transfer is happening in these connection pipes, and all the other settings, such as regarding to friction, was set as default values.

2.4. Expansion valve and control system

Expansion after the condenser is modelled with ‘Local restriction (2P)’ -block. In the block the pressure is decreased as the fluid goes through the restriction. There are two options for the pressure loss model: Control volume and Bernoulli, out of which Control volume option is used. Mass balance is kept throughout the expansion and energy flow rates also stay the same at the inlet as well as at the outlet because the expansion is assumed to be adiabatic. The restriction area is given as an input for the block, and its value is controlled by a PI control system.

Opening area was determined based on the superheat temperature after the evaporator as this is a typical way of controlling the expansion valve. The valve operation is thus similar as Thermostatic Expansion Valve (TEV). [15] The controlled parameter could also have been chosen to be pressure after the evaporator but the superheat was chosen as this way fluid entering the compressor will always be in vapor phase. PI controller uses inputs of proportional and integral values. The values were chosen by initial testing with the goal being finding values which made the control’s ability to change the system prompt. Proportional value of 1E-4 and integral value of 1E-5 produced sufficient response time into the control system and were therefore used. Expansion valve control system is shown in Fig. 2.

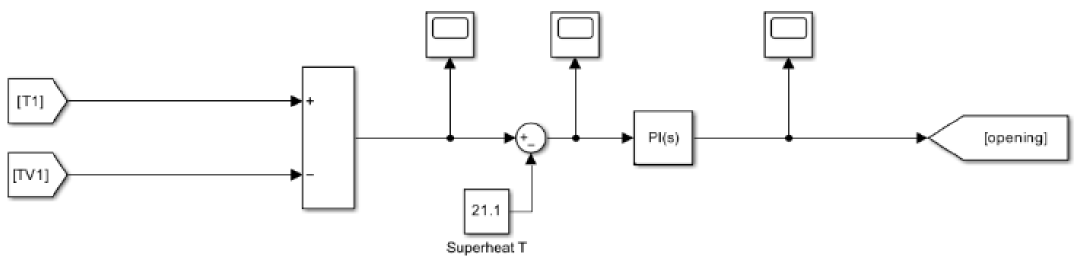

Figure 2. Expansion valve control.

Superheat is measured in the system by subtracting saturation temperature from the fluid temperature after the evaporator. The target for the amount of superheat is set as constant, in this case as 21.1 K. The error signal sent to the PI controller is thus the difference between the measured and targeted superheat values. The signal sent to the valve opening then corresponds to the changes made by the controller.

Other control was done with the compressor in similar fashion. The rotational speed of compressor shaft is changed based on the corresponding mass flow rate. For this control system proportional value of 0.5 and integral value of 0.1 were used. Rotational speed control is shown in Fig. 3.

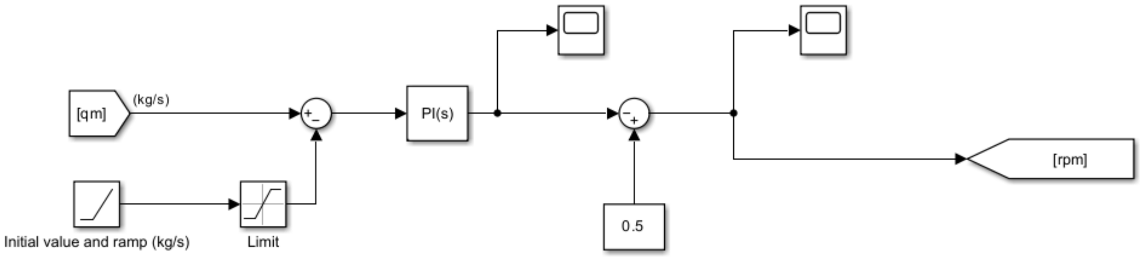

Figure 3. Compressor rotational speed control

One difference between these two control systems is that rotational speed control needed an extra part after the PI controller in order to operate correctly. The signal received from PI controller is subtracted from given constant, 0.5 value. Without this the calculation would get stuck in the beginning of the simulation. The value chosen for this should be of a similar magnitude to the signal leaving the control system, which in this situation is at a magnitude of one.

2.5. Simulation

Simulations were run for 1000 seconds. Used solver was 'daessc' which is the differential algebraic equation solver in Simscape. Initilization of the blocks was done by setting initial pressure and vapor quality on the model blocks. The pressures were set to the same value as they are in the measurements. Vapor quality value was set similarly as estimation of the components value in the measurements. For example, in evaporator and condenser it was set as 0.5 while in pipes it was either 0 or 1 depending on the location of the pipe in the cycle. At midpoint of the simulations, at 500 second time stamp the refrigerant mass flow target in the control system was changed from 2.2 kg/s to 1.4 kg/s. This way the system has to change from a stationary state and some dynamic behavior can then be seen.

The boundaries between the low temperature cycle and its adjacent cycles were at the condenser and evaporator. Inflows from the outer cycles into these heat exchangers were set at constant temperatures, pressures and flow rates. At the outlets only the pressures were set while temperatures then changed depending on the heat transfer rate from one fluid to the other. These constant values were directly taken from the steady state measurement data. Important inputs of the main components in the system are shown in Table 2.

Table 2. Inputs for main components in the simulation.

	Unit	Value
Initial refrigerant mass flow	kg/s	2.2
Volumetric flow in heat source cycle	l/s	22.36
Mass flow in intermediate cycle	kg/s	30.0
Heat source inlet temperature	°C	22.4
Heat source inlet pressure	bar	3.41
Heat source outlet pressure	bar	2.97
Intermediate cycle inlet temperature	°C	48.9
Intermediate cycle inlet pressure	bar	3.0
Intermediate cycle outlet pressure	bar	2.5
Compressor nominal mass flow rate	kg/s	2.2
Compressor nominal shaft speed	rpm	3600
Compressor isentropic efficiency	-	0.7
Compressor nominal volumetric efficiency	-	0.95
Compressor nominal pressure ratio	-	3.7
Compressor nominal inlet pressure	bar	2.7
Compressor nominal inlet temperature	°C	26.8
Compressor mechanical efficiency	-	0.9
Number of plates	-	23
Plate length	m	1.2
Plate width	m	1.2
Spacing between plates (condenser)	m	0.003
Spacing between plates (evaporator)	m	0.0025
Surface area enlargement factor (Evaporator)	-	1.2
Surface area enlargement factor (Condenser)	-	1.6
Friction factor (Heat exchangers)	-	1.7
Loss coefficient for port manifolds	-	1.5

3. Results and Discussion

Results achieved from simulating the low temperature cycle are presented and discussed here. Figs. 4-7 are used to visualize some dynamic effects of the system, and they show the monitored parameters during the simulation. The simulated mass flow and the control system input signal are plotted as function of simulation time in Fig. 4. At first the cycle has mass flow of 2.2 kg/s and after the change the mass flow is 1.4 kg/s.

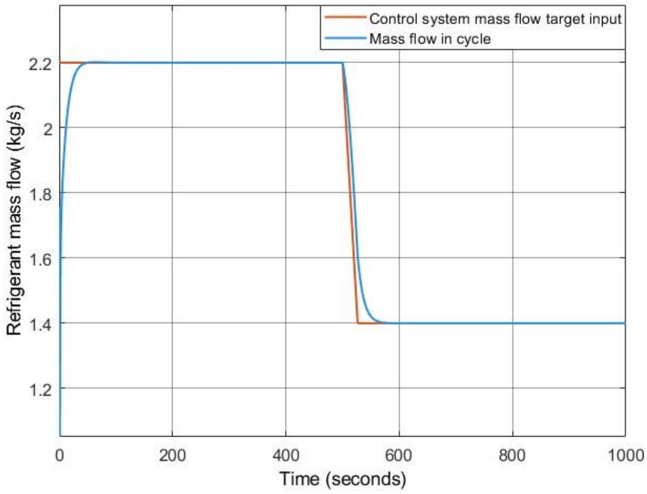

Figure 4. Refrigerant mass flow and the controller mas flow input signal during simulation.

The plot shows how quickly the mass flow rate in the cycle responded to the change in target mass flow input signal. Duration of the step change was set as 30 seconds, change started at time step of 500 s and the signal reached 1.4 kg/s limit at 530 s. During this change the lag between the real mass flow and control input value is quite small, which means that the mass flow control is working promptly. It is worth pointing out now that the chosen control parameters and logic is not the same as is used in the real facility operations, as that would require more information on the system and some transient operation data. Therefore, the dynamic response achieved shows a theoretical response, not necessarily what the real system would give out. Condenser heating power and compressor mechanical power, as well as their corresponding Coefficient of Performance (COP) are plotted as function of time in Fig.5.

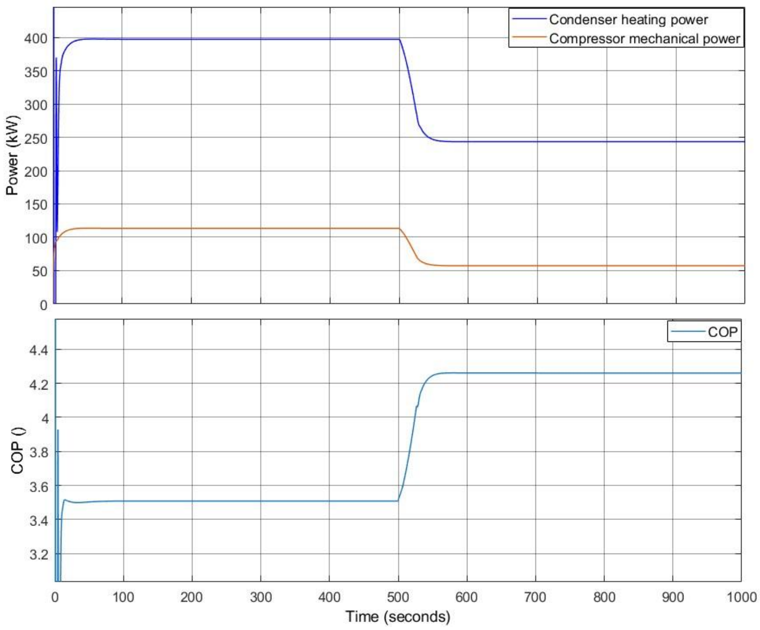

Figure 5. Compressor mechanical power, condenser heating power and COP during simulation.

The power and COP plots change as the mass flow changes. When the mass flow is reduced the powers also decrease. However, the COP increased as the refrigerant mass flow rate was decreased. Reason for this is that the compressor mechanical power decreases more in proportion to its initial value than the condenser heating power. Fig. 6 presents the monitored pressure at different places of the cycle and Fig. 7 includes the p-h diagram for the cycles at stationary states.

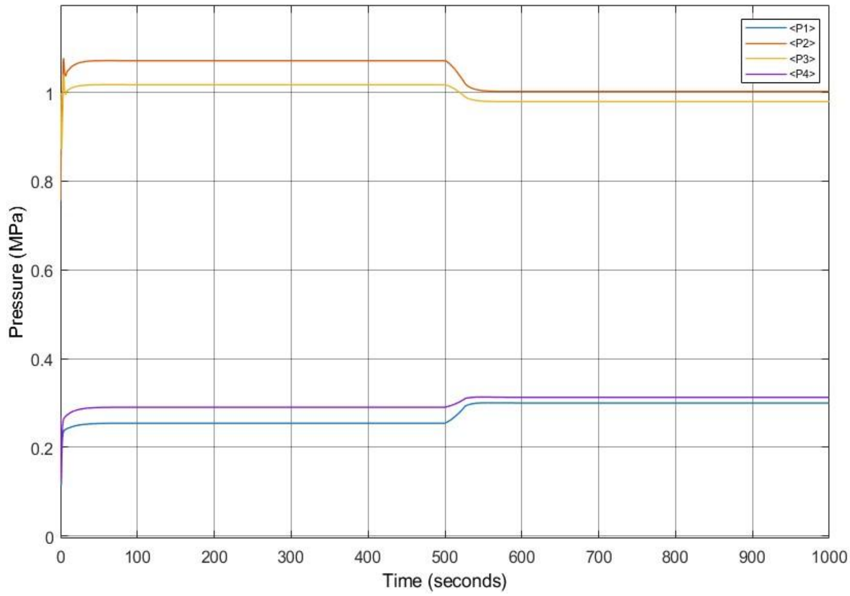

Figure 6. Pressure at different points in the cycle during simulation.

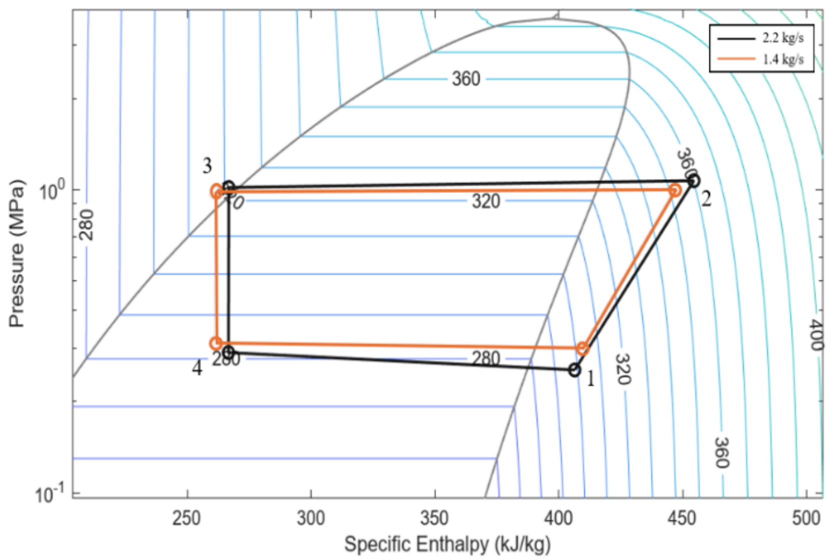

Figure 7. p-h diagram of the cycle with different mass flows.

With reduction in mass flow the cycle sets on stationary state in which the pressure ratio of the compressor is decreased as can be seen from the figures above. The decrease is about 26.5 %. Other noticeable change is that with higher mass flow rate the pressure losses in evaporator and its adjacent pipes is clearly more drastic than with the lower mass flow cycle, and that in lower mass flow cycle subcooling is happening more. This, of course, is due to the IHX and subcooler heat flow rates, which stayed constant throughout the simulation, as with lower mass flow rate the heat transfer rate would also be reduced. Comparison of simulation results and the data from measurements is presented for a stationary operating point with 2.2 kg/s refrigerant mass flow rate in Table 3.

Table 3. Simulation results and measured data comparison.

	Simulation	Measured data	Percentage Difference [%]
p_1 [bar]	2.5	2.7	7.4
p_2 [bar]	10.7	10.0	7.0
p_3 [bar]	10.2	9.6*	6.25
p_4 [bar]	2.9	3.0*	3.3
Φ_{cond} [kW]	397	390	1.8
Φ_{evap} [kW]	300	290	3.4
P_{comp} [kW]	113	99	14.1
T_1 [°C]	25.5	26.8	4.9
T_2 [°C]	87.1	73.8	18.0
T_3 [°C]	48.0	42.4	13.2
T_4 [°C]	8.4	7.2*	16.7
$\dot{m}_{refr}$ [kg/s]	2.2	2.2	0.0
COP [-]	3.5	3.9	10.3

* Estimated, not taken from direct measurements.

Comparing the simulated and measured values in Table 3, there are some quite clear deviations between them. The heat powers deviate only a couple of percentages, pressures deviate a bit more and most temperatures as well as compressor power deviate the most, over 10 % at minimum. The way the compressor was modelled is one major source of these differences. Temperature after the compressor is significantly higher in simulation than in measurements. This higher temperature will then affect rest of the cycle as the temperatures at these points are also higher than they should be. Reason for this is the choice of compressor parameters such as the isentropic efficiency.

It was noticed during build-up of the model that the choice of isentropic efficiency of compressor has a great effect on the compressor output, such as the power and outlet temperature, and this way it also affects the COP. The cause of COP rise in Fig. 5. is most likely due to constant isentropic enthalpy used in the compressor model. As the operating conditions change, the isentropic efficiency will also change, but now it is forced to stay constant. That is why the value should be chosen as accurately as possible, to present the behavior of the real compressor unit. In this simulation the used value did not match the efficiency of the real compressor at the chosen operational conditions which is why a more fitting value should have been used. Because the analytical method for efficiency specification was used in the model, the isentropic efficiency stayed constant, but for more detailed modeling it can be switched to tabulated. This tabulated method would take data sets of isentropic efficiency, pressure ratio and rotational shaft speed and interpolate the isentropic efficiency as function of the other two parameters.

What should also be noted is that the received measurement data of the heat pump cycles didn't have all the necessary points available. For example, there was no data on pressure measurements at the points between condenser and evaporator, and therefore some of the pressure values needed to be estimated. In Table 3 all the points which were estimated are marked with '*'. Pressures were estimated from the pressure losses reported in heat exchanger manufacturer's datasheets, and temperature T_4 was then calculated using these pressures and the other known values. Briefly explained, the estimation was done so that the pressure loss was assumed to change according to the mass flow change. As the used mass flow rate was lower than in the datasheet's case, the pressure loss was also assumed to decrease proportionally. T_4 was then calculated with usage of CoolProp by using the estimated pressures and the known temperature and specific enthalpy values at the evaporator outlet, as well as the heat transfer rate into the evaporator. It is also important to point out that the accuracy of the measurements is not considered here, and therefore the presented measured values can have some uncertainties.

4. Conclusions

In this paper a simple dynamic model for large-scale heat pump system was developed. The studied case had a cascade type of heat pump but only the low temperature cycle was considered in simulation. Ready-made physical simulation components of Simscape were used in generating the model in MATLAB Simulink environment. The achieved results were evaluated against measured data from an operational industrial heat pump system, with the comparison performed at steady state conditions. The simulated results show good agreement with the measured values. This is satisfactory as the goal of this model wasn't to yet give exact results, but just to be able to operate dynamically – switch from one operational point to another – and to mimic the stationary operation with adequate accuracy. Capability of the model to operate under dynamic conditions was also tested, by adjusting the cycle refrigerant mass flow rate. This showed the models capability to properly adjust to the changing operating conditions as well as provided information that the selected control strategy is feasible for the studied system.

Due to simplifications made in this model, some major phenomena were left out of consideration. Most noteworthy simplification was that thermal mass of the system was ignored. However, as it is one of the most, if not the most important phenomenon in the heat pump system determining how quickly the system can change from one stationary condition to another, it should be considered in accurate simulations. Therefore in future work the generated model will be enhanced by having the model consider this thermal inertia either by utilizing ready-made Simscape components or by generating an improved heat exchanger component code for it. Additionally next steps should also include advancing the model in order to model the whole cascade heat pump system so that the dynamics of this kind of more complex heat pump systems could be studied. In the future a longer operating period for the whole system will be modeled and compared to the measured values under fluctuating conditions. With an accurate model, the dynamics of a heat pump system and their capabilities to operate in flexible ways can be assessed. Model presented in this paper is yet unable to be operated accurately in this way, but it can and will be used as a stepping stone in making an applicable model in the future.

Nomenclature

A	Surface area	[m^2]
b	Spacing between plates	[m]
β	Chevron angle	[deg]
C	Clearance volume fraction	[-]
c_1, c_2, c_3	Constants	[-]
D	Diameter	[m]
$\dot{E}$	Energy flow rate	[W]
f	Friction factor	[-]
h	Specific enthalpy	[kJ/kg]
k	Thermal conductivity	[W/mK]
L	Length	[m]
$\dot{m}$	Mass flow	[kg/s]
N	Number	[-]
Nu	Nusselt number	[-]
P	Power	[W]
Pr	Prandtl number	[-]
Re	Reynolds number	[-]
S	Flow cross-sectional area	[m^2]
U	Convective heat transfer coefficient	[W/m^{2}K]
V	Volume	[m^3]
W	Width	[m]
x	Vapor fraction	[-]
Δ	Change	[-]
Φ	Heat power	[W]
ϕ	Area enlargement factor	[-]
ξ	Loss coefficient	[-]
η	Efficiency	[-]
ρ	Density	[kg/m^3]
v	Specific volume	[m^3/kg]
ω	Angular velocity	[rad/s]

Subscripts

cond	Condenser
disp	Displacement
evap	Evaporator
f	Fluid

h	Hydraulic
i	Internal node
in	Inlet
nom	Nominal
out	Outlet
p	Plate
port	Port at inlet and outlet
refr	Refrigerant
SL	Saturated liquid
SV	Saturated vapor
t	Total
V	Volumetric
Acronyms	
COP	Coefficient of Performance
TEV	Thermal Expansion Valve

Acknowledgements

Authors would like to thank Lempäälän Lämpö oy for co-operation and providing necessary information. The paper was financially supported by a project which is funded by Business Finland. Project in question is "Flexible Energy Systems, Value for Flexibility (V4F)".

References

[1] EU. 2019. Going climate-neutral by 2050 : a strategic long-term vision for a prosperous, modern, competitive and climate-neutral EU economy.. Publications Office. doi:10.2834/02074.

[2] Eurostat. 2025. Electricity and heat statistics. Available: https://ec.europa.eu/eurostat/statistics-explained/index.php?title=Electricity_and_heat_statistics#Derived_heat_production

[3] Rosenow, J., Arpagaus, C., Lechtenböhmer, S., Oxenaar, S. Pusceddu, E. 2025. The heat is on: Policy solutions for industrial electrification. *Energy Research & Social Science*. Vol. 127. doi: https://doi.org/10.1016/j.erss.2025.104227.

[4] Schibuola, L., Scarpa, M., & Tambani, C. 2015. Demand response management by means of heat pumps controlled via real time pricing. *Energy and Buildings*, Vol. 90, p. 15-28. https://doi.org/10.1016/j.enbuild.2014.12.047

[5] Jiménez-Arreola, M., Wieland, C., & Romagnoli, A. 2017. Response time characterization of Organic Rankine Cycle evaporators for dynamic regime analysis with fluctuating load. *Energy procedia*, Vol.129, p. 427-434. https://doi.org/10.1016/j.egypro.2017.09.131

[6] Kim, J. H., Kim, T. S., & Ro, S. T. 2001. Analysis of the dynamic behaviour of regenerative gas turbines. *Proceedings of the Institution of Mechanical Engineers, Part A: Journal of Power and Energy*, Vol. 215, p. 339-346. https://doi.org/10.1243/0957650011538569

[7] Koury, R.N.N., Faria, R.N., Nunes, R.O., Ismail, K.A.R, Machado, L. 2013 Dynamic model and experimental study of an air-water heat pump for residential use. *International Journal of refrigeration*. Vol. 36, p. 674-688. https://doi.org/10.1016/j.ijrefrig.2012.11.006

[8] Mortada, S., Zoughaib, A., Clodic, D., Arzano-Daurelle, C. 2012 Dynamic modeling of an integrated air to- air heat pump using modelica. *International journal of refrigeration*. Vol. 35, p. 1335-1348. https://doi.org/10.1016/j.ijrefrig.2012.03.009

[9] Wolscht, L., Knobloch, K., Jacquemoud, E., & Jenny, P. 2024. Dynamic simulation and experimental validation of a 35 MW heat pump based on a transcritical CO2 cycle. *Energy*, Vol.*294*, 130897. https://doi.org/10.1016/j.energy.2024.130897

[10] Chamoun, R., Rulliere, R., Haberschill, P., Berail, J. F. 2012 Dynamic model of an industrial heat pump using water as refrigerant. *International Journal of refrigeration*. Vol. 35, p. 1080-1091. https://doi.org/10.1016/j.ijrefrig.2011.12.007

[11] Ko, J., Takata, N., Thu, K., Miyazaki, T. 2020. Dynamic modeling and validation of carbon dioxide heat pump system. *EVERGREEN Joint Journal of Novel Carbon Resource Sciences & Green Asia Strategy*, Vol. 7 p.172-194. https://doi.org/10.5109/4055215

[12] Singh, S., & Sørensen, K. 2018. Dynamic model of a heat pump based house heating system. In *59th SIMS Conference on Simulation and Modelling*. Vol. 153, pp. 87-94. Linköping University Electronic Press. https://doi.org/10.3384/ecp1815387

[13] Bell, I. H., Wronski, J.T, Quoilin, S., Lemort, V. 2014 Pure and Pseudo-pure Fluid Thermophysical Property Evaluation and the Open-Source Thermophysical Property Library CoolProp. *Industrial & Engineering Chemistry Research*. Vol. 53, p. 2498-2508, https://doi.org/10.1021/ie4033999

[14] The MathWorks, Inc. 2025. Simscape Fluids. Available: https://se.mathworks.com/help/hydro/index.html?s_tid=CRUX_lftnav

[15] Elliott, M., Walton, Z., Bolding, B., & Rasmussen, B. P. 2009. Superheat control: A hybrid approach. *HVAC&R Research*, Vol. 15, p. 1021-1043. https://doi.org/10.1080/10789669.2009.10390877